10th World Congress on Structural and Multidisciplinary Optimization
May 19 -24, 2013, Orlando, Florida, USA

OPTIMIZATION OF THE NANO-SECOND PULSED LASER ABLATION PROCESS USING FINITE ELEMENT ANALYSIS

Jaeyeol Lee[1] and Jeonghoon Yoo[2]

[1] Graduate School of Mechanical Engineering, Yonsei University, Seoul, Korea, leedream77@yonsei.ac.kr
[2] School of Mechanical Engineering, Yonsei University, Korea, Seoul, yoojh@yonsei.ac.kr

1. Abstract
We try to simulate the ablation process using nano-second pulsed laser. In case of ablation by the nano-second pulsed lasers, the energy transfer process is similar to the general heat transfer process, so the process can be simulated by the basic heat conduction theory. We have performed the finite element analysis in various cases and compared results with pre-existing experiments qualitatively for process parameters such as laser fluence, pulse width and beam spot size. To control the ablation process as desired, the relation between results such as ablation depth, width or efficiency and process parameters should be verified. Finally, the optimized process condition is obtained using the design of experiment (DOE) and response surface methodology (RSM).

2. Keywords: Laser ablation, Design of experiment, Finite element analysis

3. Introduction
The laser ablation is one of precision machining processes using the high energy of focused laser beam. With various advantages, the laser ablation is widely used in industry and it can be applied to machining processes such as drilling, cutting, marking, welding, etc. For laser ablation process, pulsed laser is generally used. Depending on the type of pulsed laser, analyzing method may be changed. In the case of femto-second or pico-second laser, the ablation process would be not simple, because of the shockwave effect, phase explosion; therefore, thermal non-equilibrium should be taken into account. However, the ablation process using nano-second laser could be analyzed in the concept of general heat conduction theory [1] and laser beam absorbed in material surface would be treated as a heat source. To simulate ablation process effectively, various parameters such as laser fluence, wavelength, pulse width, spot size and shot numbers are considered and the relation between those parameters and ablation results must be verified. Finally, the optimal process condition would be set based on the relation.

In many previous studies, they are dealing with the nano-second laser ablation process but most of those studies are experimental researches [2, 3]. Though some studies are based on numerical analysis, it is restricted to one-dimensional (1D) or two-dimensional (2D) analysis and dealing with a few parameters [4-7]. In this research, not only the geometry of the material but also the laser heat source is considered in three-dimensional (3D) space. Because the laser source is modeled reflecting the Gaussian distribution and absorption coefficient of the material is taken into account, it is able to estimate the ablation efficiency or the aspect ratio of the ablation part depending on the beam spot size.

However, it is hard to simulate phase transformation process because the boundary of the material changes continuously as material is removed. Unfortunately, any finite element (FE) commercial package does not support the material removal process considering phase transformation such as solid to liquid or liquid to gas. For the purpose of making up this shortcoming, in this work, the material portion which exceeds the boiling temperature is considered as gas and laser heat source changes in accordance with the material boundary shift.

Figure 1 shows the procedure considering material boundary and heat source variation. The FE analysis is conducted using a commercial package DEFORM v.10.2.1 combined with additional FORTRAN programs. As you can see in Fig. 1 (a), as the material absorbs laser beam energy, temperature increases and soon exceeds the boiling temperature. Then, these materials are treated as gas, and the boundary surface changes as displayed in Fig. 1(b). Simultaneously, shape of the laser heat source changes according to the material geometry because initial surface which incident laser meets varies. Through repeated ablation processes, the material removal process with phase transformation can be analyzed effectively.

.

4. Background theory
As previously mentioned, nanosecond laser ablation process can be interpreted by general heat conduction theory, and the governing analysis equation is expressed as in Eq. (1).

(a) (b)

Figure 1: Geometrical change of the material surface heated by laser beam

$$\rho C_p \frac{\partial T}{\partial t} + \nabla \cdot (-k \nabla T) = Q \tag{1}$$

The properties of the heat source Q depend on laser power, reflectivity of the material, absorption coefficient, and geometrical distribution of the laser beam [6]. It is expressed as in Eq. (2).

$$Q = (1 - R) P \alpha I \tag{2}$$

where α is the absorption coefficient of the material. The laser beam is not only absorbed at the surface, but also it penetrates through the material. The energy absorbed by the material is exponentially decreased according to the vertical depth. Considering the characteristic, laser becomes a 3D heat source, not a 2D surface heat source. A vertical intensity distribution of *I* is expressed as follows:

$$I = I_0 e^{-\alpha z} \tag{3}$$

As previously mentioned, the horizontal distribution of the intensity *I* has a Gaussian distribution. The distribution depends only on the full width at the half maximum (FWHM). As you can see in Fig. 2, the intensity has the value of 1 at the center of laser beam and it decreases exponentially through the distance from the beam center. It is expressed as in Eq. (4).

$$I = I_p \exp\left(-x^2 \Big/ 2\left(\frac{FWHM}{2\sqrt{2\ln(2)}}\right)^2 \right) \tag{4}$$

Equations above describe fundamental properties of the laser and nano-second laser ablation process. Based on the equations, both two and three dimensional FE analysis considering various parameter conditions are carried out and both parameter study and optimization are conducted.

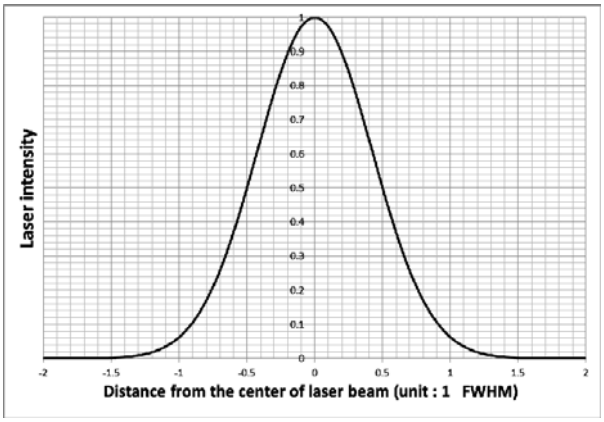

Figure 2: Gaussian distribution of the laser intensity according to the horizontal distance

5. Modeling and result

5.1. Modeling

The 3D model is as described in Fig. 3. The laser irradiating region has a circular shape of diameter 3μm and it is the same as FWHM previously defined. Heat transfer with surrounding air can be ignored because the analysis time is too short for meaningful heat exchange. As described in Fig. 4, convective heat transfer does not affect

temperature change. Also, flow effect due to molten material and laser absorption of the vaporized material are ignored. Silicon (Si) material is used for analysis. It has thermal conductivity of 149 W/(m·K), specific heat of 703(J·K)/kg, density of 2330Kg/m^3, and boiling point 700K. Therefore, the element whose temperature exceeds 700K is set to be air. Figure 5 shows the effect of phase transition. The material considering phase transition has the higher maximum temperature than the model that ignores the effect.

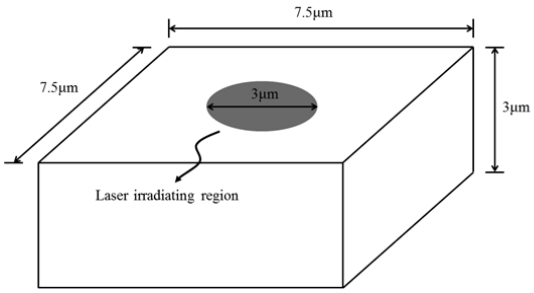

Figure 3: Simulation model composed of Si material

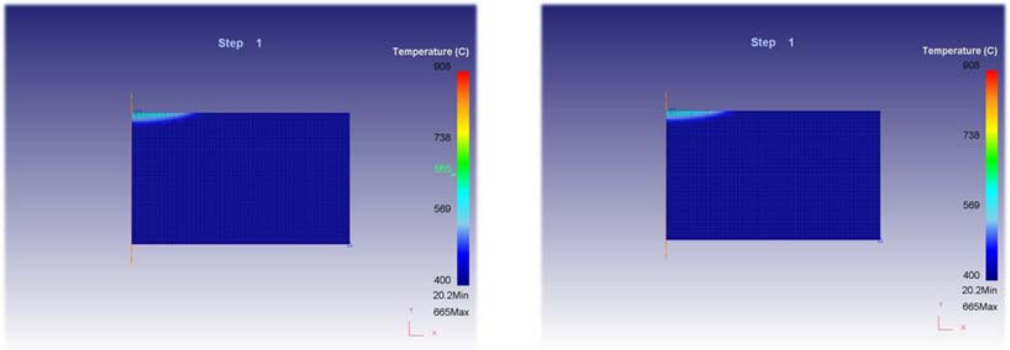

(a) (b)

Figure 4: Simulation result Comparison: (a) considering and (b) ignoring convective heat exchange

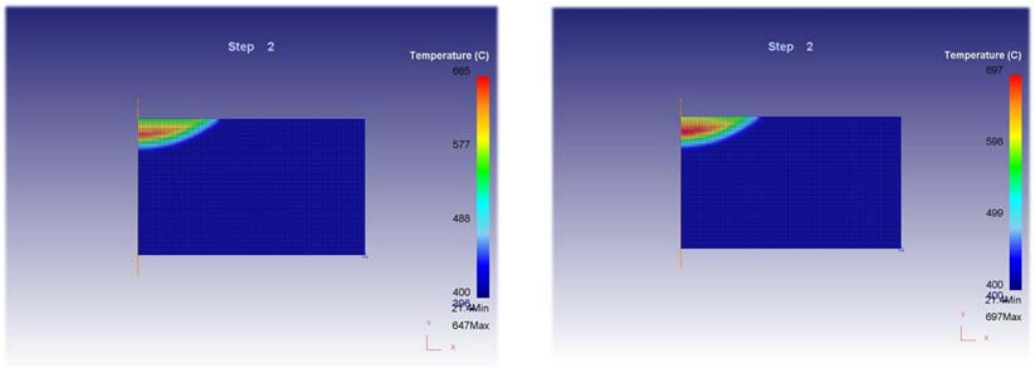

(a) (b)

Figure 5: Maximum temperature of two different models; (a) model ignoring phase transition at temperature 665K (b) Phase transition model at maximum temperature 697K

5.2. Numerical Simulation Results

To confirm the relation between process parameters and ablation condition, the parameter study is carried out. Simulation is conducted using both two and three dimensional model and both are described. The purpose of the parameter study is to confirm the relation between each parameters and compare the result with previous experiment results qualitatively. Generally, in case of 2D simulation, it has the higher temperature than 3D model

analysis case, because the simulation result is dependent on the mesh size.

Figure 6 shows that the hole size of the removed material expands as the laser is repeatedly shot on the material. The Simulation result is verified by comparison with the experimental study in a previous work [4]. Figure 7 shows that the volume of removed material is proportional to the laser fluence, and it is similar to the result of previous experimental work [3].

Figure 8 shows that the removed volume is dependent on the wavelength of the input laser. As the wavelength varies, the reflectivity of the material also changes. In the case of Si material, the reflectivity decreases as the wavelength increases and the removed volume increases at the same time. Although the absorption coefficient varies according to the wavelength change, it is small enough to be ignored compared to effect of reflectivity changes. So, only the reflectivity change is considered.

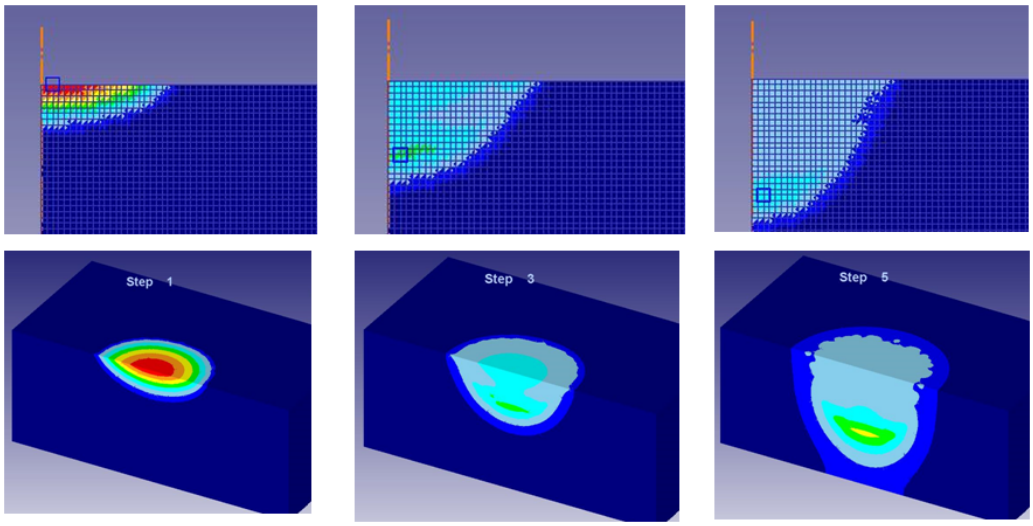

Figure 6: Distribution of ablated material after repeated laser shot by 2D and 3D simulation result

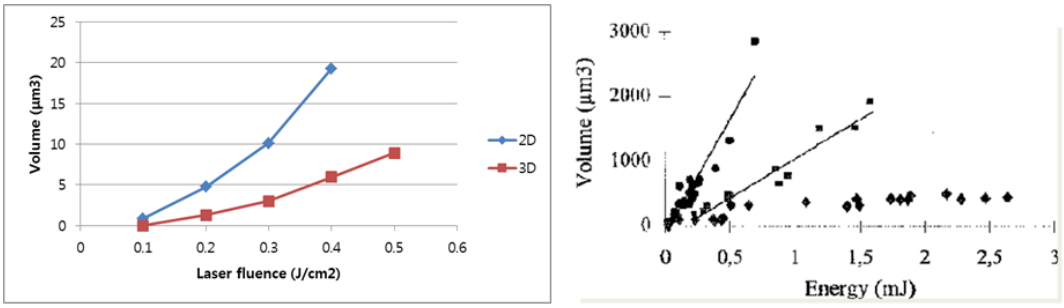

(a) (b)

Figure 7: Removed volume change by changing the laser fluence; (a) by simulation and (b) by experiment [3]

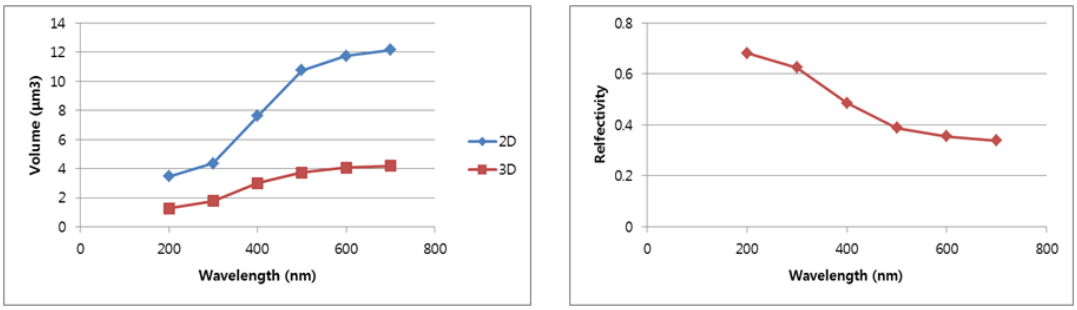

Figure 8: Removed volume and reflectivity variation due to the wavelength change

Finally, the relation between the removed volume and the laser pulse width is verified. Figure 9 shows that removed volume increases as the pulse width decreases. As the pulse width decreases, the same energy of laser is focused within a short duration. As a result, laser intensity increases at the same time.

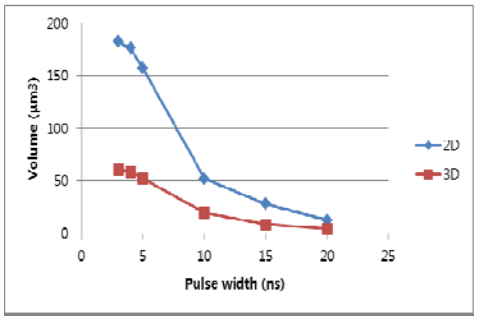

Figure 9: Effect of the pulse width on the removed volume

6. Parameter optimization

Based on the numerical simulation result, parameter optimization for the ablation process is carried out. To determine the optimal parameter value, DOE is conducted. Among various parameters, the laser fluence, the laser spot size and the pulse width were chosen to control parameters. The laser spot size is defined as FWHM. An objective of the ablation process is defined as a combination of removed volume and aspect ratio. The aspect ratio is defined as the width divided by the height of the removed material shape. Therefore, the objective function of the process can be expressed as in Eq. (5).

$$Maximize \quad F = w\frac{Y_1}{Y_{01}} + (1-w)\frac{Y_2}{Y_{02}} \tag{5}$$

Here, Y_1 is the removed volume and Y_2 means the aspect ratio. Y_{01} and Y_{02} are the values of the removed volume and the aspect ratio of the initial model, respectively. The initial model has 0.25 J/cm^2 laser fluence, 15ns pulse width and 3.5μm spot size. w is the weighting factor for two different objectives.

By the simulation result, response surfaces of the Y_1 and Y_2 are derived as in Eqs. (6) and (7), respectively. $x1$, $x2$ and $x3$ denote the laser fluence, the pulse width and the spot size, respectively. Constraints of the control parameters are described as $0.2 \le x_1 \le 0.3$, $20 \le x_2 \le 30$ and $3 \le x_3 \le 4$. Equations (6) and (7) have the adjust R-square values of 0.988 and 0.8422, respectively, so it is concluded that both response surfaces are sufficiently reliable. Using those response surface regression functions, the Pareto optimal relation is derived and it is displayed in Fig. 10. As described in the figure, in the case of weighting factor at 0~0.1, optimized values of $x1$, $x2$ and $x3$ are 0.2, 20 and 3 and in the case of weighting factor of 0.2~1, optimized values are 0.3, 30 and 4. Results are shifting from a constraint boundary to the opposite boundary rapidly and no intermediate values are pointed.

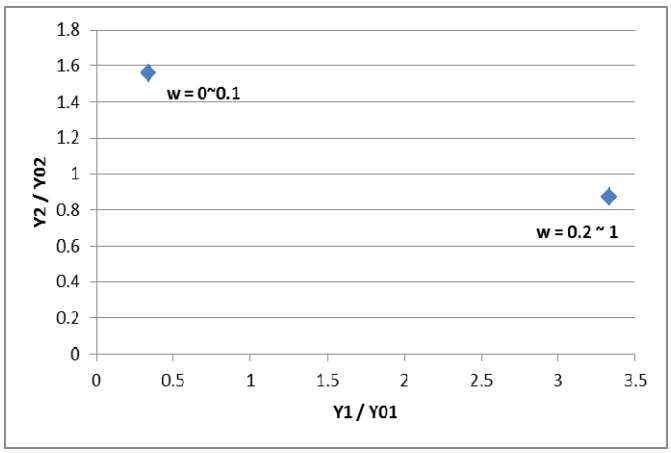

Figure 10: Pareto optimal graph

$$Y_1/Y_{01} = 4.70878 - 19.5209 \cdot x1 + 0.142799 \cdot x2 - 2.70005 \cdot x3 + 10.0328 \cdot x1^2 + 0.00585208 \cdot x2^2 + 0.393856 \cdot x3^2 - 0.568228 \cdot x1 \cdot x2 + 9.06636 \cdot x1 \cdot x3 - 0.0779086 \cdot x2 \cdot x3 \quad (6)$$

$$Y_2/Y_0 = 3.30561 - 24.3205 \cdot x1 + 0.183403 \cdot x2 - 0.237279 \cdot x3 + 12.5761 \cdot x1^2 - (3.33671/10000) \cdot x2^2 - 0.00595487 \cdot x3^2 + 0.0563368 \cdot x1 \cdot x2 + 3.82792 \cdot x1 \cdot x3 - 0.0446428 \cdot x2 \cdot x3 \quad (7)$$

where $0.2 \le x_1 \le 0.3$, $20 \le x_2 \le 30$, $3 \le x_3 \le 4$

7. Conclusion

In this study, the nano-second pulsed laser ablation process is analyzed based on the general heat conduction theory. The relation between various parameters and the ablation process is derived by both 2D and 3D FE analysis using DEFORM v10.2.1. In addition, the relation is compared with pre-existing experimental results and it is verified that the simulation has a similar tendency with experiments. Using the simulation method, the DOE procedure of the ablation process is conducted and optimized values of control parameters are derived.

8. Acknowledgement

This work was supported by National Research Foundation of Korea (NRF) grant funded by the Korea government (MEST) (No. 2012-0005701).

9. References

[1] H. Kim, Various laser applications, *Inter-vision*, Seoul, Korea, 2006.

[2] N. M. Bulgakova and A.V. Bulgakov, Pulsed laser ablation of solids: transition from normal vaporization to phase explosion. *Applied Physics A*, 73 (2), 199-208, 2001.

[3] A. Semerok, C. Chaléard, V. Detalle, J. L. Lacour, P. Mauchien, P. Meynadier, C. Nouvellon, B. Sallé, P. Palianov, M. Perdrix and G. Petite, Experimental investigations of laser ablation efficiency of pure metals with femto, pico and nanosecond pulses, *Applied Surface Science*, 138-139, 311-314, 1999.

[4] B. Oh, Y. Jung, N. Kim and D. Kim, Analysis of sapphire micro-drilling by a nano second visible laser pulse, *Journal of Korean Society of Laser Processing*, 12 (1), 7-13, 2009.

[5] B. Oh and D. Kim, Numerical simulation of nanosecond pulsed laser ablation in air, *Journal of Korean Society of Laser Processing*, 6 (3), 37-45, 2003.

[6] H. S. Lim and J. Yoo, FEM based simulation of the pulsed laser ablation process in nanosecond fields, *Journal of Mechanical Science and Technology*, 25 (7), 1911-1816, 2011.

[7] J. K. Chen, J. E. Beraun, L. E. Grimes and D. Y. Tzou, Modeling of femtosecond laser-induced non-equilibrium deformation in metal films, *International Journal of Solids and Structures*, 39 (12), 3199-3216, 2002.